RAPID COMMUNICATIONS

PHYSICAL REVIEW C VOLUME 48, NUMBER 1 JULY 1993

Measurement of the magnetic form factor of the neutron

P. Markowitz,[1] J. M. Finn,[1] B. D. Anderson,[2] H. Arenhövel,[3] A. R. Baldwin,[2] D. Barkhuff,[4] K. B. Beard,[1,13] W. Bertozzi,[5] J. M. Cameron,[6] C. C. Chang,[7] G. W. Dodson,[5] K. Dow,[5] T. Eden,[2] M. Farkhondeh,[5] B. Flanders,[8] C. Hyde-Wright,[9] W.-D. Jiang,[9] D. Keane,[2] J. J. Kelly,[7] W. Korsch,[5] S. Kowalski,[5] R. Lourie,[4] R. Madey,[2,13] D. M. Manley,[2] J. Mougey,[10] B. Ni,[6] T. Payerle,[7] P. Pella,[11] T. Reichelt,[12] P. M. Rutt,[1] M. Spraker,[6] D. Tieger,[5] W. Turchinetz,[5] P. E. Ulmer,[10] S. Van Verst,[4] J. W. Watson,[2] L. B. Weinstein,[5,*] R. R. Whitney,[10] and W. M. Zhang[2]

[1]*The College of William and Mary, Williamsburg, Virginia 23185*

[2]*Kent State University, Kent, Ohio 44242*

[3]*Johannes Gutenberg-Universität, D-W-6500 Mainz, Germany*

[4]*University of Virginia, Charlottesville, Virginia 22904*

[5]*Massachusetts Institute of Technology and Bates Linear Accelerator Center, Cambridge, Massachusetts 02139*

[6]*Indiana University Cyclotron Facility, Bloomington, Indiana 47408*

[7]*University of Maryland, College Park, Maryland 20742*

[8]*The American University, Washington, D.C. 20016*

[9]*University of Washington, Seattle, Washington 98195*

[10]*CEBAF, Newport News, Virginia 23606*

[11]*Gettysburg College, Gettysburg, Pennsylvania 17325*

[12]*Physikalisches Institut Universität Bonn, 5300 Bonn, Germany*

[13]*Hampton University, Hampton, Virginia 23668*

(Received 5 October 1992)

The ^{2}H$(e,e'n)^1$H quasielastic cross section was measured at Q^2 values of 0.109, 0.176, and 0.255 (GeV/c)^2. The neutron detection efficiency was determined by the associated particle technique with the ^{2}H(γ,pn) reaction for each of the three neutron kinetic energies. These ^{2}H$(e,e'n)$ measurements of the coincidence cross sections are the first at low Q^2. The cross sections are sensitive primarily to the neutron magnetic form factor G_M^n at these kinematics. The extracted G_M^n values have smaller uncertainties than previous data and are consistent with the dipole parametrization at the two higher momentum transfers; at the lowest momentum transfer, the value of G_M^n is $\sim$10% higher than the dipole value.

PACS number(s): 13.40.Fn, 14.20.Dh, 25.10.+s, 25.30.Fj

The magnetic form factor of the neutron, G_M^n, has been the subject of extensive study for many years [1–7]. This fundamental observable is the Fourier transform of the neutron current distribution in the Breit frame. The magnetic form factor at $Q^2=0$ is defined to be the magnetic moment μ_n with a known value of $-1.913\,042\,7(5)$ nuclear magnetons [8]. At nonzero momentum transfers the knowledge is much less precise; the uncertainty in $(G_M^n)^2$ is typically of the order of 20% [9] and becomes even larger for Q^2 above 1–2 (GeV/c)^2. Lacking a suitable free neutron target, Hofstadter first suggested quasielastic electron scattering from deuterium to measure electromagnetic properties of the neutron, such as the size of the magnetic moment cloud [10]. This Rapid Communication reports a refinement of Hofstadter's method: a coincidence experiment to measure the quasielastic ^{2}H$(e,e'n)^1$H cross section and extract the magnetic form factor of the neutron. In comparison with prior data, smaller total uncertainties in G_M^n result from these first exclusive measurements at $Q^2=0.109$, 0.176, and 0.255 (GeV/c)^2 and from the first measurement of the neutron detection efficiency with the ^{2}H(γ,pn) reaction. The data reported here show an enhancement at low Q^2 of G_M^n relative to the dipole value, G_D, given below.

The electromagnetic form factors of the nucleon are fundamental quantities that must be described accurately before any model of baryon structure can be considered successful. The connection between models that postulate confinement and the underlying theory of QCD at low Q^2 is crucial but still contentious. Knowledge of the electromagnetic form factors is important also for testing nuclear models [11]; for example, calculations of cross sections and polarization observables in deuteron electrodistintegration are sensitive to these form factors [12]. A new generation of experiments exploiting polarization observables plans to measure interference terms between the relatively large magnetic form factors and smaller electric [13] and strange [14] form factors. The current knowledge of G_M^n limits the ability to extract precise values of these smaller form factors [15].

Previous measurements of G_M^n were performed primarily by either ^{2}H(e,e') inclusive experiments [1–3], ^{2}H$(e,e'\bar{p})$ anticoincidence measurements [4,5], or ^{2}H$(e,e'n)$ coincidence experiments [6,7]. Because the first method relies on subtracting the proton part of the cross section, it requires good knowledge of the deuteron

*Presently at Old Dominion University, Norfolk, Virginia 23529.

wave function; additionally, it requires performing a longitudinal-transverse separation, which demands careful control of systematic uncertainties. The second method, wherein one detects an electron and does not detect a coincident proton, also requires knowledge of the deuteron wave function and careful attention to the proton detection efficiency to account for all processes whereby one might not see the coincident proton. The ^{2}H$(e,e'n)$ coincidence method was used twice before, but only at high momentum transfers $[Q^2 \geq 0.39(\mathrm{GeV}/c)^2]$. The advantage of an electron-neutron coincidence measurement is that it eliminates the large quasifree scattering contribution from the proton. The major difficulty in ^{2}H$(e,e'n)$ coincidence measurements is obtaining an absolute calibration of the efficiency for detecting neutrons. The two prior coincidence experiments determined the efficiency by the associated particle technique with the reaction $\gamma p \rightarrow \pi^+ n$; the present experiment utilizes the reaction $\gamma d \rightarrow pn$ for the first time.

The experiment took place at the Bates Linear Accelerator Center with apparatus developed to measure G_E^n, the electric form factor of the neutron [16]. Whereas G_E^n was determined by measuring the polarization of neutrons scattered by polarized electrons, G_M^n was determined by measuring the unpolarized cross section. Electrons scattered quasielastically from deuterium were detected in the One-Hundred-Inch Proton Spectrometer (OHIPS) [17]. The coincident neutrons were detected at a fixed neutron angle of 57° in a sequential array of four mineral-oil scintillators [16] with a mean geometric solid angle of 9.67 msr. The neutron array was situated inside a shielding enclosure with a front face of 10 cm of lead sandwiched between two 3.18-cm steel plates. The roof and sides were composed respectively of 0.61- and 1.22-m slabs of reinforced high-density ($\rho = 3.9$ g/cm^3) concrete. OHIPS used a small (2.48 msr) circular collimator that made the results insensitive to the details of the electron transport optics; i.e., the electron acceptance was purely geometrical. The electron scattering angles were 47.0°, 42.0°, and 37.0° for incident energies of 444, 636, and 868 MeV, respectively.

During replay, the OHIPS momentum acceptance (±4.4% in hardware) was restricted to ±2.0% in software. This restriction limited the recoil momentum range sampled to an rms value of about 20 MeV/c and limited the focal plane of OHIPS to a region where the acceptance is uniform. Together with the small collimator, this software restriction also constrained the kinematics to illuminate only the central part of the neutron detector, thereby minimizing edge effects in the neutron detector. (The yield at the edges of the detector was down by over an order of magnitude as compared to the yield at the center of the neutron detector.) The Q-system developed at LAMPF was used for data acquisition. Prescaled single-arm data and coincidence data were taken simultaneously. The prescaled data were useful in verifying the geometric acceptance of OHIPS from elastic ^{1}H(e,e) scattering and in the measurements of the neutron detection efficiency, as discussed below.

The liquid-deuterium target cell was a cylinder, 5.06 cm in diameter, with an elgiloy wall thickness of 50.8 μm. The cell was maintained at a nominal temperature of 21 K and at a pressure above the saturation curve. The average current was 0.5 μA with a duty factor of 1%. Luminosity studies under experimental conditions determined that the maximum observed variation in density was 1% with beam on target; temperature gradients within the cell were estimated to be less than 1% effect. The contribution from the empty cell was less than 0.25% in the single-arm spectrum and insignificant in the coincidence yield. The same cell was used also for the hydrogen calibration runs. Hydrogen data were taken at the two extreme kinematics; the results were interpolated to give the results at the intermediate point.

Measurement of the ^{2}H$(e,e'n)^1$H cross section relies on knowledge of the neutron detection efficiency, $\varepsilon(P_n)$, where P_n is the neutron momentum. This efficiency is in turn the product of the transmission $T(P_n)$ of neutrons through the shielding wall and the probability $\rho(P_n)$ that the scintillators will detect an incident neutron. We used the ^{2}H(γ,pn) reaction to determine the product $\varepsilon = T\rho$ via the associated particle technique. This technique requires that both a neutron and an associated charged particle be produced in a nuclear reaction with a two-body final state. The efficiency is defined as the ratio of the coincidence cross section to the single-arm proton cross section. Protons from the reaction ^{2}H(γ,pn) were detected in OHIPS with its polarity reversed, and the fraction of the associated neutrons detected in coincidence determined the efficiency. These measurements of the neutron detection efficiency are independent of the efficiency of the spectrometer for protons. Because pion production was forbidden kinematically, the gamma-ray energy could be inferred from the measured quantities. Although the neutron detection efficiency depends upon the choice of software threshold, the efficiency-corrected cross sections were the same within uncertainties for three threshold values of 4±2 MeV (electron equivalent). This result confirms the internal consistency of the efficiency calibration. The efficiency measurement utilized a single electron beam energy of 254 MeV. The neutron detector remained at the 57° angle, whereas the proton angle was adjusted so that the kinetic energies of the neutrons matched the central kinematic values used in the experiment.

The bremsstrahlung photons incident on deuterium give a different neutron population, both in terms of energy and angular distributions, from the cross section measurement. (The efficiency measurements resulted in a smaller spread in neutron kinetic energy than the cross section measurements). Software cuts were placed on the proton angle and momentum to ensure the angular distribution of neutrons was the same during the calibration as it was during the cross section measurement. However, the efficiency changes slowly over the acceptances as a function of energy. The three measurements of the efficiency could then be further used to produce a map of neutron efficiency versus kinetic energy of the neutron. This map was put into the Monte Carlo, to determine the effect (event by event) of the changes in efficiency. Offsets in the code were used to determine the sensitivity of the cross section to experimental misalignments in the kine-

TABLE I. Summary. The cross section uncertainty is ± statistical ± systematic. The extracted G_M^n uncertainty is ± statistical ± systematic ± theoretical.

Q^2 (GeV/c)^2	0.109	0.176	0.255
ε	4.46%	5.84%	7.23%
Radiative corrections	1.25	1.23	1.25
σ_{Meas} (nb/MeV sr^2)	34.6±1.3±1.5	27.3±0.5±1.2	24.0±1.1±0.8
Arenhövel model of σ	26.8	25.3	22.7
Factorized model of σ	26.7	25.2	22.3
$\Delta G_M^n/G_M^n$ from knowledge of G_E^n	±0.0075	±0.011	±0.018
$\Delta G_M^n/G_M^n$ from nucleon-nucleon potential	±0.010	±0.010	±0.0095
Extracted $G_M^n/\mu_N G_D$	1.136±0.022±0.025±0.014	1.039±0.010±0.026±0.015	1.028±0.025±0.021±0.021

matics.

A potential source of background arises from the conversion of quasielastically scattered protons to neutrons in the two-step process ^{2}H$(e,e'p)$-(p,n). This effect was measured with a hydrogen target by looking for coincident neturons resulting from reactions in the lead-steel wall of the shielding enclosure for the neutron detector. These reactions yielded a flat background in the time-of-flight spectrum. The contribution to the cross section was determined to be negligibly small ($<0.5\%$). This measurement also verified that the veto counters and the shielding were working properly; charged particles were not mistakenly identified as neutrons.

The uncertainty in the luminosity arises from an uncertainty of ±1% in the target thickness, ±1% due to temperature gradients in the target, and ±0.5% uncertainty in the integrated current [18]. Ray-tracing codes established that the electron solid angle was equal to the geometrical solid angle of the collimator. The single-arm measurement for $p(e,e)$ agreed with the known cross section [19] to better than 1%, which confirmed that the electron detection efficiency was unity within the uncertainties from proton form factors [19], luminosities, and radiative corrections. The statistical uncertainty contains both the uncertainty from fitting the time-of-flight peak and the uncertainty from the number of counts in that peak.

Table I summarizes the experimental results. The value of G_M^n was extracted by comparing the measured cross section to Arenhövel's [12] theoretical cross section for a given value of G_M^n averaged over the experimental acceptances. Arenhövel assumed the Galster parametrization [20] for G_E^n, the dipole parameterization for G_M^n, and the Paris nucleon-nucleon potential. The theoretical cross section took into account meson-exchange currents (MEC), final-state interactions (FSI), and isobar configurations (IC). As might be expected at the top of the quasielastic peak, the inclusion of these terms made only a small difference to the cross sections ($\sim 1\%$ at the highest momentum transfer to less than 3% at the lowest momentum transfer). The sensitivity of the cross section to FSI in various nucleon-nucleon potentials was explored for the Bonn, Argonne V14, Nijmengen, and the Paris for our kinematics [12]; the cross sections differ by $\leq 2\%$ (and the form factor by $\leq 1\%$), with the Paris potential giving intermediate values. [Note that the use of a different model of the electric form factor would result in a different value of the extracted magnetic form factor. The contribution of the Galster parameterization [20] of G_E^n to the cross section ranges from 1.5% at $Q^2=0.109$ (GeV/c)^2 to 3.5% at $Q^2=0.255$ (GeV/c)^2. The uncertainty in G_E^n was taken to be ±100%. The theoretical uncertainty in the extracted value of G_M^n results from a combination of uncertainties in G_E^n and the nucleon-nucleon potential.]

The Monte Carlo program MCEEP [21] was used to average each theoretical cross section over the experimental acceptances, and the output was compared with our measured cross section after applying radiative corrections. Response-function components of the cross section were computed for a grid of points covering the experimental acceptances. This grid was calculated for various values of the neutron magnetic form factor. Interpolated values of the response functions were then used event by event to simulate the "averaged" cross section for our finite acceptances. Sensitivity to kinematic uncertainties was examined by varying the kinematics in the Monte Carlo simulation and examining the change in the cross section. The uncertainty from a 1-msr offset in the electron angle was determined to be small ($\leq 0.1\%$). An offset in the electron energy of ±0.5% reduces the cross section by 2%. The uncertainties in the neutron detection efficiency, the empty-target subtraction, and the hydrogen (p,n) contamination were dominated by statistics. The contributions to the uncertainty in the measured cross sections are summarized in Table II.

TABLE II. Cross section uncertainties (%).

Q^2 (GeV/c)^2	0.109	0.176	0.255
Empty target	±0.2	±0.1	±0.3
(p,n) reactions	±0.9	±1.4	±1.4
Target thickness	±1.4	±1.4	±1.4
Beam current	±0.5	±0.5	±0.6
Solid angle	±0.6	±0.6	±0.6
Scattering angle	±0.02	±0.1	±0.03
Energy	±2.0	±2.0	±2.0
Neutron detection efficiency	±3.4	±3.6	±1.7
Radiative corrections	±2.5	±2.3	±2.5
Total systematic uncertainty	±5.0	±5.2	±4.2
Statistical uncertainty	±4.0	±1.9	±4.9

Radiative corrections for the electron emitting a real photon before or after interacting with the neutron were calculated by comparing the yield for the theory without radiation to the yield for the theory with radiation in the peaking approximation [22]. The low-energy cutoff for the neutron kinetic energy in the radiative correction was 30 MeV. A factorized cross section [23] along with a fit to the previously measured momentum distribution [24] were used (because the correction requires knowing the cross section over a broad kinematical range) within the program MCEEP. The deviations between this factorized model and the Arenhövel model [12] are small ($<1\%$) for the kinematics of interest. The uncertainty in the radiative correction was estimated to range between 2.3% and 2.5% of these kinematics.

The most common form-factor parametrization is the empirical dipole fit, G_D, given by

$$G_D = \left[1+\frac{Q^2}{0.71\ (\mathrm{GeV}/c)^2}\right]^{-2} = G_E^p = \frac{G_M^p}{\mu_p} = \frac{G_M^n}{\mu_n}\ .$$

Results of our measurements of $(G_M^n)^2$ in units of $(\mu_n G_D)^2$ are plotted as solid circles in Fig. 1 versus Q^2; all uncertainties were added in quadrature to determine the total uncertainty (displayed in Fig. 1). Plotted uncertainties from prior experiments are published values, which are not always directly comparable to those from this work. The uncertainties in the inclusive data of Grossetête *et al.* [2] and Braess *et al.* [3], the anticoincidence data of Hanson *et al.* [4] and Budnitz *et al.* [5], and the coincidence data of Barten *et al.* [6] and Stein *et al.* [7] do not include a theoretical uncertainty. It should be noted that the uncertainties in the inclusive data of Hughes *et al.* include a global 5% theoretical uncertainty [1]. The experiments differ as well in the detail with which systematic uncertainties are treated.

The dot-dashed curve labeled "Mainz" in Fig. 1 is an empirical fit [19] of the nucleon magnetic form factor to proton scattering data. The dashed curve labeled "Gari-Krümpelman" [25] is a semiphenomenological synthesis of meson and quark dynamics, and the short-dashed curve labeled "Höhler" [26] is based on an extended model of vector dominance. Common theoretical parametrizations of G_M^n tend to underestimate the data at low Q^2. The dipole form factor describes the global data set in a reasonable fashion, as indicated by previous results at high Q^2 [27]. New results from the NE11 Collaboration reduce the uncertainty at higher Q^2 [28]; however, the low-Q^2 data indicate that this simple dipole prescription

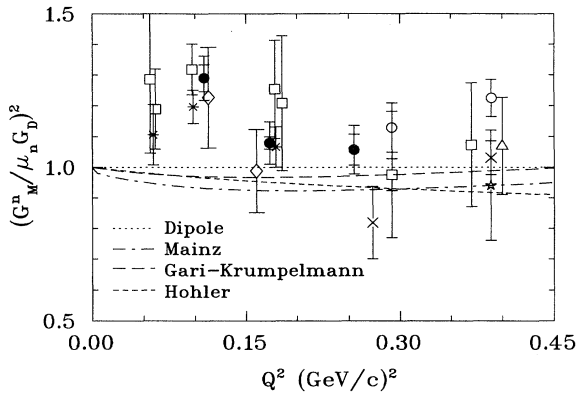

FIG. 1. The square of the neutron magnetic form factor $(G_M^n)^2$, in units of the dipole value $(\mu_n G_D)^2$ versus Q^2. The inner (outer) error bars on the solid circles are statistical (total) uncertainties from the present work. The hollow squares are from Hughes *et al.* [1], the diamonds are from Grossetête *et al.* [2], the asterisks are from Braess *et al.* [3], the ×'s are from Hanson *et al.* [4], the hollow circles are from Budnitz *et al.* [5], the stars are from Bartel *et al.* [6], and the triangles are from Stein *et al.* [7]. The text describes the fits. The data of Hughes *et al.* and Braess *et al.* have been displaced slightly to improve readability.

is inadequate to describe the detailed behavior of the form factor. The present measurements clearly indicate an enhancement at low Q^2 of G_M^n relative to the dipole fit and the other fits in Fig. 1, which substantiate previous indications from inclusive measurements. Although we attribute this excess strength to an enhanced form factor, it could be due also to nuclear effects not incorporated into standard models; either case is interesting. Additional measurements in this region would be useful to confirm this results and to determine its full momentum-transfer dependence.

We would like to thank the staff at the Bates Linear Accelerator Center for their efforts. This work was supported in part by the National Science Foundation under Grants Nos. PHY-91-12816, PHY 91-07064, HRD-91-54090, PHY-89-02479, PHY-89-18491, and PHY-86-58127, by the Department of Energy under Grants Nos. DE-FG05-90ER40570, DE-FG06-90ER40537, DE-FG02-89ER40531, and DE-AC02-76ER03069, and by grants from the Deutsche Forschungsgemeinschaft (SFB 201 and RE 791/1-1).

[1] E. B. Hughes *et al.*, Phys. Rev. **139**, B458 (1965); *ibid.* **146**, 973 (1966).
[2] B. Grossetête, S. Julian, and P. Lehmann, Phys. Rev. **141**, 1435 (1966).
[3] D. Braess, D. Hasselmann, and G. Kramer, Z. Phys. **198**, 527 (1967).
[4] K. M. Hanson *et al.*, Phys. Rev. D **8**, 753 (1973).
[5] R. J. Budnitz *et al.*, Phys. Rev. **173**, 1357 (1968).
[6] W. Bartel *et al.*, Phys. Lett. **30B**, 285 (1969); *ibid.* **39B**, 407 (1972); Nucl. Phys. **B58**, 429 (1973).
[7] P. Stein *et al.*, Phys. Rev. Lett. **16**, 592 (1966).
[8] Particle Data Group, K. Hikasa *et al.*, Phys. Rev. D **45**, S1 (1992).
[9] I. Sick, Nucl. Phys. **A497**, 379c (1989).
[10] R. Hofstadter, Rev. Mod. Phys. **28**, 214 (1956).
[11] B. Blankleider and R. M. Woloshyn, Phys. Rev. C **29**, 538 (1984).
[12] H. Arenhövel, W. Leidemann, and E. L. Tomusiak, Z.

Phys. **331**, 123 (1988); **334**, 363(E) (1989); W. Leidemann, K.-M. Schmitt, and H. Arenhövel, Phys. Rev. C **42**, R826 (1990); H. Arenhövel, private communication.

[13] R. Madey, contact person, Reports Nos. Bates E89-04 and CEBAF E89-005; D. Day, contact person, Report No. CEBAF E89-018.

[14] D. H. Beck, contact person, Report No. Bates E89-06; P. A. Souder, contact person, Report No. CEBAF E91-010; E. Beise, contact person, Report No. CEBAF E91-004; D. H. Beck, contact person, Report No. CEBAF E91-004.

[15] A. K. Thompson *et al.*, Phys. Rev. Lett. **68**, 2901 (1992).

[16] R. Madey *et al.*, IEEE Trans. Nucl. Sci. **36**, 231 (1989); R. Madey *et al.*, in *Proceedings of The Conference on Intersections Between Particle and Nuclear Physics,* Tucson, 1991, edited by Willem T. H. van Over, AIP Conf. Proc. No. 243 (AIP, New York, 1991), p. 954

[17] R. S. Turley, Ph.D. thesis, M.I.T., 1984, unpublished.

[18] P. Dunn, Nucl. Instrum. Methods **165**, 163 (1979).

[19] G. G. Simon *et al.*, Nucl. Phys. **A333**, 381 (1980); G. G. Simon *et al.*, *ibid.* **A364**, 285 (1981).

[20] S. Galster *et al.*, Nucl. Phys. **B32**, 221 (1971).

[21] P. E. Ulmer, MCEEP: Monte Carlo for Electro-Nuclear Coincidence Experiments, Report No. CEBAF-TN-91-101 (1991).

[22] L. W. Mo and Y. S. Tsai, Rev. Mod. Phys. **41**, 205 (1969).

[23] T. De Forest, Nucl. Phys. **A392**, 232 (1983).

[24] F. Krautschneider, Ph.D. thesis, Bonn University, Report No. BONN-IR-76-37, 1976.

[25] M. Gari and A. Krümpelmann, Z. Phys. A **322**, 689 (1986).

[26] G. Höhler *et al.*, Nucl. Phys. **B114**, 505 (1976).

[27] S. Rock *et al.*, Phys. Rev. Lett. **49**, 1139 (1982).

[28] A. Lung *et al.*, Phys. Rev. Lett. **70**, 718 (1993).